www.lajss.org
Latin American Journal of Solids and Structures 3 (2006) 263–278

Anisotropic damage in composite shell structures

Roberto C. Pavan* and Guillermo J. Creus

CEMACOM-PPGEC-UFRGS, Porto Alegre – RS – Brazil

Abstract

Continuum Damage Mechanics (CDM) had important developments since the initial works of Kachanov and Rabotnov, and constitutes now a practical tool to account for macrocospic damage in materials and structures. In this work, an application of the anisotropic damage theory based in Murakami work is presented. In the presented formulation, the fourth order damage tensor M (that relates Cauchy and effective stress tensors) is determined on the basis of the tensor Ω (three-dimensional area density of damage) that, in turn, can be determined through experimental data. The analytical formulation is set in incremental form and implemented into a finite element program (for plates and shell structures in composite material) taking account of geometrically non-linear effects. In order to verify and validate the numerical model, comparisons between analytical and experimental results for simple situations are presented.

Keywords: anisotropic damage, composite materials, finite elements, progressive failure.

1 Introduction

Anisotropy is an important characteristic of composite materials, that must be taken into account both in elastic and inelastic analysis, including damage. In this work a computational model is presented, based on damage mechanics [5, 10, 12, 13, 18, 19, 21] to simulate the progressive failure of composites under high loads. Being a micromechanical model, it allows the determination of the composite damage based on damage models for the constituents (fiber and matrix). The formulation is incorporated into a program of finite elements that can analyze plate and shell structures. The parameters of the material are determined on the basis of experimental tests and individually adjusted, and numerical results are compared with experimental data. The study is addressed to shells of fiber reinforced composite materials with polymeric matrix and set in a context of finite displacements with small strains.

The content of the paper is as follows. Section 2 presents the finite element model and the procedures for the incremental numerical solution [16, 20]. In section 3 the formulation used is presented. Using micromechanics this formulation is applied to composite materials in section 4. In section 5 some examples are shown comparing numerical and experimental results and in section 6 the conclusions are presented.

*Corresp. author email: pavan@ppgec.ufrgs.br Received 18 May 2006; In revised form 14 Aug 2006

Note: tensors are represented, according to convenience, in matrix or inditial notation. The operations with matrices have been carried through using the mathematical software MAPLE.

2 Finite element model

We follow the general procedure described in [4], including the effects of viscoelastic and hygrothermal deformations. According to reference [16] this leads to an incremental relation of the form

$$\left(\left[{}^{k}_{0}K_L \right] + \left[{}^{k}_{0}K_{NL} \right] \right) \{U\} = \left\{ {}^{k+1}P \right\} - \left\{ {}^{k}_{0}F \right\} + \{ {}_0F^v \} + \left\{ {}_0F^T \right\} + \left\{ {}_0F^H \right\} \tag{1}$$

where $\left[{}^{k}_{0}K_L \right]$ e $\left[{}^{k}_{0}K_{NL} \right]$ are the linear and non-linear tangent stiffness matrices, respectively, corresponding to step k, $\left\{ {}^{k+1}P \right\}$ is the vector of external nodal forces at step $k+1$, $\left\{ {}^{k}_{0}F \right\}$ is the vector of nodal point forces equivalent to the element stresses at the step k and, finally, $\{ {}_0F^v \}$,$\left\{ {}_0F^T \right\}$ and $\left\{ {}_0F^H \right\}$ are the vectors of viscoelastic, thermal and hygroscopic loads, respectively.

2.1 Numerical Solution

The numerical solution of the equations in (1) is implemented through an incremental-iterative procedure. Both the Newton–Raphson Method and the Generalised Displacement Control Method proposed by [25] have been implemented.

In the Newton–Raphson method, a prescribed load increment is used. One limitation of this method is the numerical instability that occurs near the limit load as the stiffness matrix becomes singular. This inconvenient is avoided by the Generalised Displacement Control Method (GDCM) in which the load increments (positive or negative) are determined for the algorithm. More details in [25].

3 Continuum damage model

3.1 Review of continuum damage mechanics

The principles of continuum damage mechanics may be introduced considering a bar subjected to a tensile force T. The uniaxial stress σ in the undamaged bar is found from the $T = \sigma A$. The original cross-sectional area A is reduced in the damaged state by the presence of voids and cracks. The effective cross-sectional area of the damaged bar is denoted by $\bar{A}$ and the effective stress is $\bar{\sigma}$. The bar in both the real and continuum damaged configurations are subjected to the same tensile force T and therefore $T = \bar{\sigma}\bar{A}$. Equating the two expression of T, one obtains the following expression for the effective uniaxial stress $\bar{\sigma}$

$$\bar{\sigma} = \frac{A}{\bar{A}}\sigma \tag{2}$$

Using the definition of the damage variable ϕ as originally proposed by Kachanov [9],

$$\phi = \frac{A - \bar{A}}{A} \tag{3}$$

and substituting into equation (2), one ontains:

$$\bar{\sigma} = \frac{\sigma}{(1-\phi)} \tag{4}$$

This idea was generalized by various authors [10, 13, 14], to multiaxial stress states and anisotropic damage.

3.2 Anisotropic damage and effective stresses

According to reference [18], for the anisotropic case, a relation between the global stress tensor σ_{ij} and the effective stress tensor $\bar{\sigma}_{ij}$ may be given by the linear transformation

$$\bar{\sigma}_{ij} = M_{ijkl}\sigma_{kl} \tag{5}$$

where M_{ijkl} is a fourth order damage effective tensor. For a generic state of strain and damage, the stress effective tensor $\bar{\sigma}_{ij}$ is usually no symmetrical. A symmetrical form for $\bar{\sigma}_{ij}$ is obtained through this equation

$$\bar{\sigma}_{ij} = \frac{1}{2}\left[\sigma_{ik}\left(\delta_{kj} - \phi_{kj}\right)^{-1} + \left(\delta_{il} - \phi_{il}\right)^{-1}\sigma_{lj}\right] \tag{6}$$

whereδ_{ij} is the delta de Kronecker. According to reference [23], for the general case of strain and damage, the damage tensor is given by:

$$[\phi_{ij}] = \begin{bmatrix} \phi_{11} & \phi_{12} & \phi_{13} \\ \phi_{12} & \phi_{22} & \phi_{23} \\ \phi_{13} & \phi_{23} & \phi_{33} \end{bmatrix} \tag{7}$$

For the case of plane stress, we have $\sigma_{33} = \sigma_{13} = \sigma_{23} = \phi_{33} = \phi_{13} = \phi_{23} = 0$ and the representation of the damage effective tensor [M] is reduced to

$$[M] = \frac{1}{\Delta}\begin{bmatrix} \psi_{22} & 0 & \phi_{12} \\ 0 & \psi_{11} & \phi_{12} \\ \frac{1}{2}\phi_{12} & \frac{1}{2}\phi_{12} & \frac{\psi_{11}+\psi_{22}}{2} \end{bmatrix} \tag{8}$$

where $\Delta = \psi_{11}\psi_{22} - \phi_{12}^2$ and $\psi_{ij} = \delta_{ij} - \phi_{ij}$.

3.3 Constitutive equations for elastic damage

The generalized Hooke law for the case of undamaged and damaged materials is given, respectively, by

$$\bar{\sigma}_{ij} = E_{ijkl}\bar{\varepsilon}_{kl} \tag{9}$$

$$\sigma_{ij} = \bar{E}_{ijkl}\varepsilon_{kl} \tag{10}$$

The elastic strain energy for the undamaged and damaged materials is defined, respectively, as

$$\bar{V} = \frac{1}{2}E^{-1}_{ijkl}\bar{\sigma}_{ij}\bar{\sigma}_{kl} \tag{11}$$

$$V = \frac{1}{2}\bar{E}^{-1}_{ijkl}\sigma_{ij}\sigma_{kl} \tag{12}$$

Using the hypothesis of the equivalent elastic energy [21] that assumes that "the elastic energy for the damaged material is equivalent to the elastic energy of the undamaged material when the stress is substituted by the effective stress", and equating equation (11) and (12) and using equation (5), we obtain

$$\bar{E}_{ijkl} = M^{-1}_{pqkl}E_{rspq}M^{-1}_{rsij} \tag{13}$$

Differentiating equation (11) with relation to $\bar{\sigma}_{ij}$ and using equations (5), (10) and (13) we obtain for the effective strain

$$\bar{\varepsilon}_{ij} = M^{-1}_{ijpq}\varepsilon_{pq} \tag{14}$$

3.4 Constitutive relations for incremental analysis

For incremental analyses in non-linear situations as described in Section 2, constitutive relations in incremental form are needed. Differentiating equation (10) with relation to the time,

$$\dot{\sigma}_{ij} = \left(M^{-1}_{pqkl}E_{rspq}M^{-1}_{rsij}\right)\dot{\varepsilon}_{kl} + \overset{\bullet}{\overline{\left(M^{-1}_{pqkl}E_{rspq}M^{-1}_{rsij}\right)}}\,\varepsilon_{kl} \tag{15}$$

$$\dot{\sigma}_{ij} = \left(M^{-1}_{pqkl}E_{rspq}M^{-1}_{rsij}\right)\dot{\varepsilon}_{kl} + \left(\left(\dot{M}^{-1}_{pqkl}E_{rspq}M^{-1}_{rsij}\right) + \left(M^{-1}_{pqkl}\dot{E}_{rspq}M^{-1}_{rsij}\right) + \left(M^{-1}_{pqkl}E_{rspq}\dot{M}^{-1}_{rsij}\right)\right)\varepsilon_{kl} \tag{16}$$

and considering that $M^{-1}_{pqkl}\dot{E}_{rspq}M^{-1}_{rsij} = 0$,

$$\dot{\sigma}_{ij} = \left(M^{-1}_{pqkl}E_{rspq}M^{-1}_{rsij}\right)\dot{\varepsilon}_{kl} + \left(\dot{M}^{-1}_{pqkl}E_{rspq}M^{-1}_{rsij} + M^{-1}_{pqkl}E_{rspq}\dot{M}^{-1}_{rsij}\right)\varepsilon_{kl} \tag{17}$$

From the symmetry of the damage tensor we obtain,

$$\dot{\sigma}_{ij} = \left(M^{-1}_{pqkl} E_{rspq} M^{-1}_{rsij}\right) \dot{\varepsilon}_{kl} + 2 \left(\dot{M}^{-1}_{pqkl} E_{rspq} M^{-1}_{rsij}\right) \varepsilon_{kl} \tag{18}$$

Using the chain rule,

$$\dot{M}^{-1}_{pqkl} = \frac{\partial M^{-1}_{pqkl}}{\partial \phi_{pq}} \frac{\partial \phi_{pq}}{\partial \varepsilon_{kl}} \dot{\varepsilon}_{kl} \tag{19}$$

Therefore,

$$\dot{\sigma}_{ij} = \left(M^{-1}_{pqkl} E_{rspq} M^{-1}_{rsij}\right) \dot{\varepsilon}_{kl} + 2 \left(\left(\frac{\partial M^{-1}_{pqkl}}{\partial \phi_{pq}} \frac{\partial \phi_{pq}}{\partial \varepsilon_{kl}} \dot{\varepsilon}_{kl} \right) E_{rspq} M^{-1}_{rsij} \right) \varepsilon_{kl} \tag{20}$$

$$\dot{\sigma}_{ij} = \left[\left(M^{-1}_{pqkl} E_{rspq} M^{-1}_{rsij}\right) + \left(2 \left(\frac{\partial M^{-1}_{pqkl}}{\partial \phi_{pq}} \frac{\partial \phi_{pq}}{\partial \varepsilon_{kl}} \right) E_{rspq} M^{-1}_{rsij} \varepsilon_{kl} \right) \right] \dot{\varepsilon}_{kl} \tag{21}$$

To obtain this relation in explicit form it is necessary to introduce a relation for the damage ϕ.

Let us see first an example for the uniaxial case. The exponential equation $\bar{E} = Ee^{-K\varepsilon}$ is used to model the degradation of the elastic modulus, K being a constant to be determined experimentally. Then, the damage coefficients are obtained by the expression [23]:

$$\phi = 1 - \sqrt{\frac{\bar{E}}{E}} = 1 - \sqrt{\frac{Ee^{-K\varepsilon}}{E}} = 1 - \sqrt{e^{-K\varepsilon}} \tag{22}$$

For the uniaxial case, (15) reduces to

$$\dot{\sigma} = \bar{E}\dot{\varepsilon} + \dot{\bar{E}}\,\varepsilon \tag{23}$$

Then,

$$\dot{\bar{E}} = \frac{\partial \bar{E}}{\partial \varepsilon} \dot{\varepsilon} = -KEe^{-K\varepsilon} \dot{\varepsilon} \tag{24}$$

and substituting in (23),

$$\dot{\sigma} = Ee^{-K\varepsilon} \left(1 - K\varepsilon\right) \dot{\varepsilon} \tag{25}$$

Figure 1 below represents the behavior of the degradation of the elastic modulus and of the damage coefficient for different values of K.

As expected, the nonlinear behavior of the proposed model can be observed. Damage coefficients present a behavior similar to that observed experimentally [23].

Example 1: plate under tension. To verify the incremental equation and the integration procedure implemented into the FE program, a plate subject to axial traction (figure 2) is analyzed. All of the layers possess equal thickness, elastic modulus $E = 200\ GPa$ and $K_{11} = 2500$.

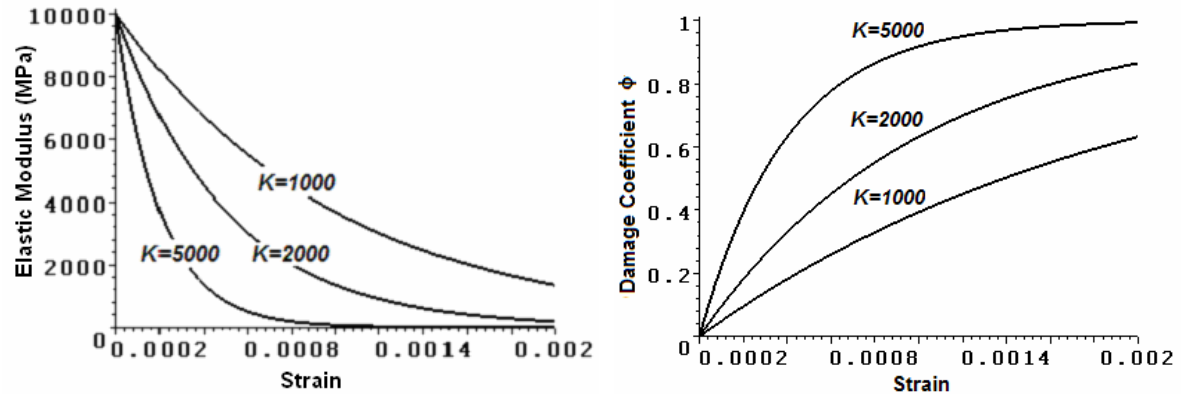

(a) (b)

Figure 1: Variation of the damage coefficient and the secant elasticity modulus with the strain. a) - Degradation of the secant elasticity module; b) - Evolution of the damage coefficient.

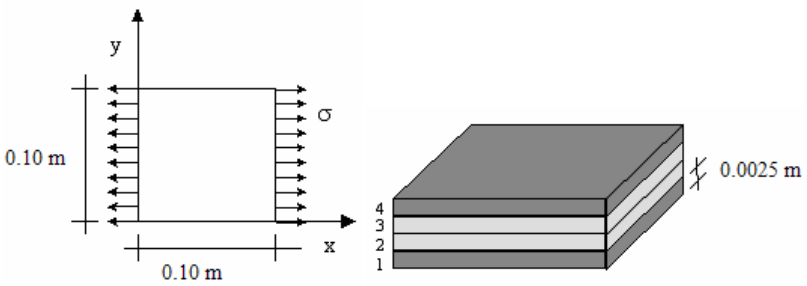

Figure 2: Geometry and loading

The numerical results obtained in the analysis are compared, in Figure 3, with the analytical expression $\sigma = Ee^{-K\varepsilon}\varepsilon$ that uses the secant modulus.

Numerical and analytical results coincide when Poisson modulus vanishes. As expected, for a Poisson modulus $\nu = 0.3$, the traverse deformation influences the behavior.

3.5 Localization and unloading.

Damage behavior has special characteristics that have to be taken into account in numerical analyses. We discuss now this point through an example.

Example 2. Non-uniform bar under tension. We consider a bar of non-uniform section and 100 mm length under tension (figure 4). The bar is modeled with two Finite Elements, using an elastic modulus $E = 18500.00\ MPa$ and a damage factor $K = 50$. Once damaged, the material remains in the damaged state under decreasing stresses. Thus, different relations have to be written for loading and unloading.

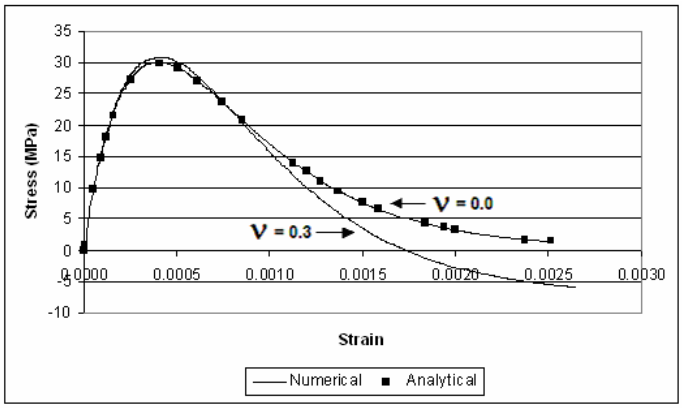

Figure 3: Relation stress x strain and incremental numeric approach

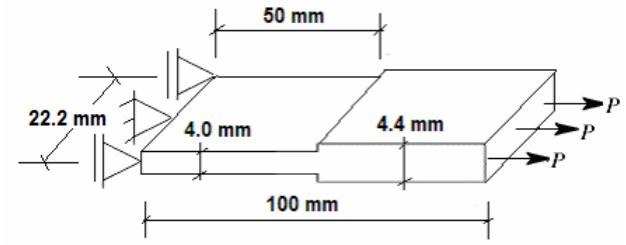

Figure 4: Geometry and loading for the nonuniform bar in tension.

Plots in Figures 5-7 show the behavior of stresses, displacements, damage and elastic modulus.

The first element, being less rigid, degrades faster and reaches the unit value of damage, where it begins to unload under increasing deformation. At this point, when it begins to unload, the damage in the second elements is about 0.3. During unloading, damage remains constant and so does the elastic modulus, which maintains the last value of the secant modulus. Thus, for loading the tangent modulus (21) is used while for unloading the secant modulus (13) is operative.

The behavior observed in this example shows that damage and strain grow always in the first element while stress and strain may diminishe in the second one. In the case of continuously varying section, he phenomenon of strain localization, characteristic of damage processes, is observed. As it is well known, this phenomenon leads to the so-called "lack of objectivity" or mesh dependence in Finite Element analyses [15].

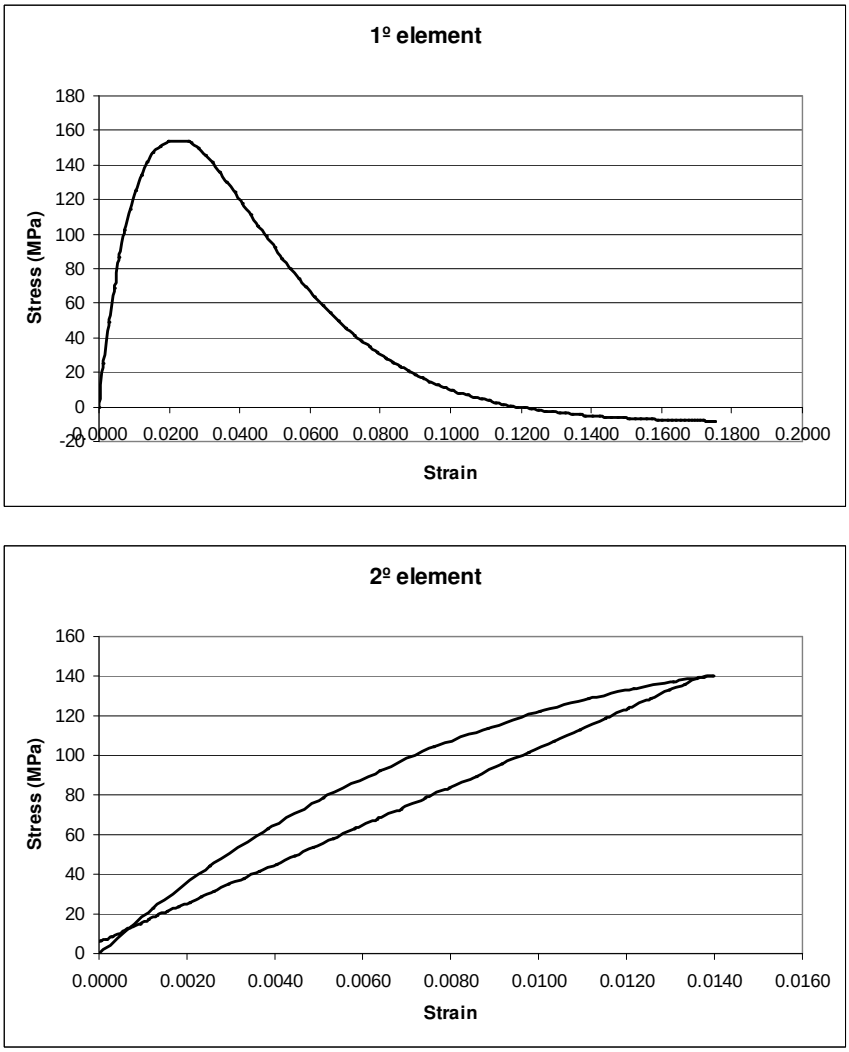

Figure 5: Stress-strain relation for the first and second elements.

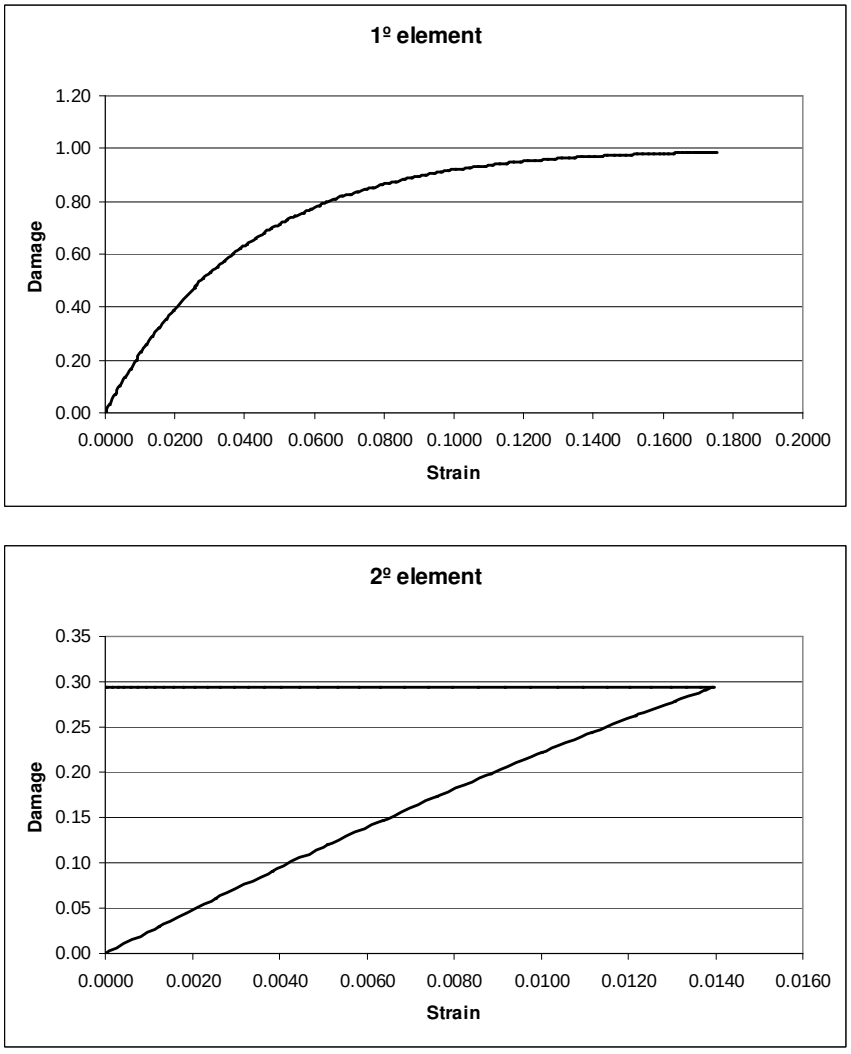

Figure 6: Damage versus strain for first and second elements.

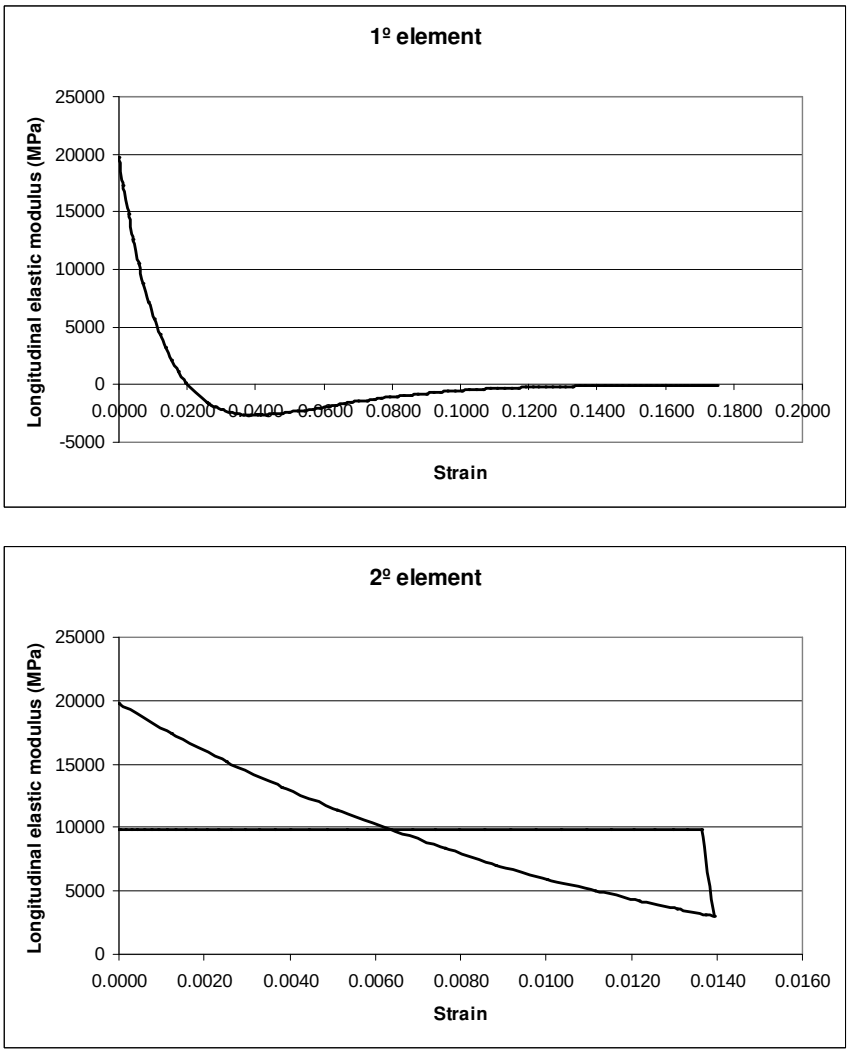

Figure 7: Elastic modulus degradation with strain for first and second elements.

4 Micromechanical characterization of damage of fiber-reinforced composite materials

4.1 Damage analysis - constitutive equations.

In the case of a composite material we can have different damage processes in the matrix and in the fiber. The present formulation allows to model each component separately and then obtain the behavior of the composite. Thus, equation (5) can be rewritten as

$$\bar{\sigma}_{ij}^{R} = M_{ijkl}^{R} \sigma_{kl}^{R} \tag{26}$$

where the index represents either the matrix (M) or the fiber (F).

The generalized Hooke law is given for each constituent as

$$\sigma_{ij}^{R} = \bar{E}_{ijkl} \varepsilon_{kl}^{R} \tag{27}$$

Again, using the hypothesis of the energy equivalence, it can be demonstrated that:

$$\bar{E}_{ijkl}^{R} = M_{pqkl}^{-R} E_{rspq}^{R} M_{rsij}^{-R} \tag{28}$$

The local stress tensor is related to the global stress tensor

$$\bar{\sigma}_{ij}^{R} = B_{ijkl}^{R} \bar{\sigma}_{kl} \tag{29}$$

$$\sigma_{ij}^{R} = \bar{B}_{ijkl}^{R} \sigma_{kl} \tag{30}$$

where B_{ijkl}^{R} is a tensor of fourth order indicating the elastic concentration factor of stresses. The relation among the damaged stress concentration tensor $\bar{B}_{ijkl}^{R}$ and the non damaged B_{ijkl}^{R} is given by:

$$\bar{B}_{ijkl}^{R} = \left(M_{ijkl}^{R}\right)^{-1} B_{ijkl}^{R} M_{pqkl} \tag{31}$$

4.2 Stress concentration tensors

In the following, the equations of Mori-Tanaka [7] are used to find the stress in the fibers. In agreement with this theory, the stresses in the fibers are equivalent to the stress obtained through an equivalent inclusion [6, 8, 11, 17, 24].

The expressions for the stress and strain concentration tensor B^{F} and A^{F} for the fibers are, respectively

$$A_{ijkl}^{F} = \left[I_{ijkl} + c^{M} S_{ijrs} E_{rsmn}^{M^{-1}} \left(E_{mnkl}^{F} - E_{mnkl}^{M} \right) \right]^{-1} \tag{32}$$

$$B_{ijkl}^{F} = \left[I_{ijkl} + c^{M} E_{ijmn}^{M} \left(I_{mnpq} - S_{mnpq} \right) \left(E_{pqkl}^{F^{-1}} - E_{pqkl}^{M^{-1}} \right) \right]^{-1} \tag{33}$$

where $[S]$ it is the Eshelby tensor (fourth order) for the elastic case, $[I]$ is the identity tensor (fourth order), c^M and c^F are the fractions of the volume corresponding, respectively, to the matrix and to the fiber.

Substituting (32) and (33) in equations (34) and (35) we obtain the stress and strain concentration tensor B^M and A^M, respectively, for the matrix:

$$c^M A^M_{ijkl} + c^F A^F_{ijkl} = I_{ijkl} \tag{34}$$

$$c^M B^M_{ijkl} + c^F B^F_{ijkl} = I_{ijkl} \tag{35}$$

Mura [17] provides the non-null components of tensor [S] for fibers with circular cross-section:

$$\begin{array}{lll} S_{1111} = \dfrac{5-4\nu^M}{8\,(1-\nu^M)} & S_{2222} = S_{1111} & S_{3333} = 0 \\ S_{1122} = \dfrac{4\nu^M-1}{8\,(1-\nu^M)} & S_{2211} = S_{1122} & S_{2323} = \dfrac{1}{4} \\ S_{2233} = \dfrac{\nu^M}{2\,(1-\nu^M)} & S_{3311} = 0 & S_{1133} = S_{2233} \\ S_{3322} = 0 & S_{1212} = \dfrac{3-4\nu^M}{8\,(1-\nu^M)} & S_{3131} = \dfrac{1}{4} \end{array} \tag{36}$$

5 Validation of the numerical analysis

Example 3. Composite under transverse compressive stress. In this example, we consider a plate under transverse compression whose material properties are given in Table 1. As the plate is subjected to stress in one direction, only one damage parameter (for each matrix and fiber) has to be determined. From the fitting of experimental results [22] we obtain $K_{22} = K^F_{22} = K^M_{22} = 20$.

Table 1: Material properties for E-Glass/ MY750/HY917/DY063

Properties	Fiber	Matrix	Laminate
Módulus E_1 (GPa)	74.0	3.35	45.6
Módulus E_2 (GPa)	74.0	3.35	16.2
G_{12}	30.8	1.24	5.83
Poisson	0.2	0.35	0.278

Example 4: Analysis of a unidirectional composite. The present formulation can be used to determine stresses in each constituent (fiber and matrix) of the composite. In this example,

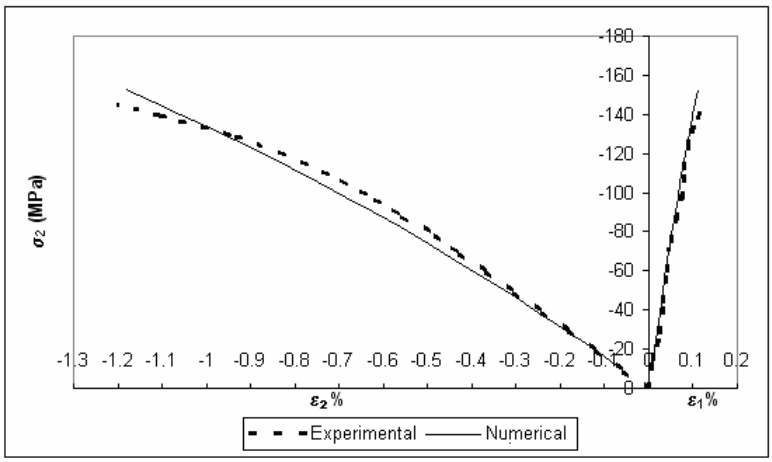

Figure 8: Transverse compressive stress/strain curve for E-glass/ MY750/HY917/DY063 epoxy lamina. Comparison of experimental and numerical values.

we consider a plate under uniaxial tension. Experimental details and mechanical properties of the materials are ($E^F = 410,000.00MPa$ e $E^M = 80,000.00MPa$) [2]. Other properties were determined using mixture theory [1]. As the plate is under axial tension, only one K_{ij} parameter for each matrix and fiber are needed: $K_{11} = K_{11}^F = K_{11}^M = 50$. In figure 9, the comparison between numerical and experimental results is shown.

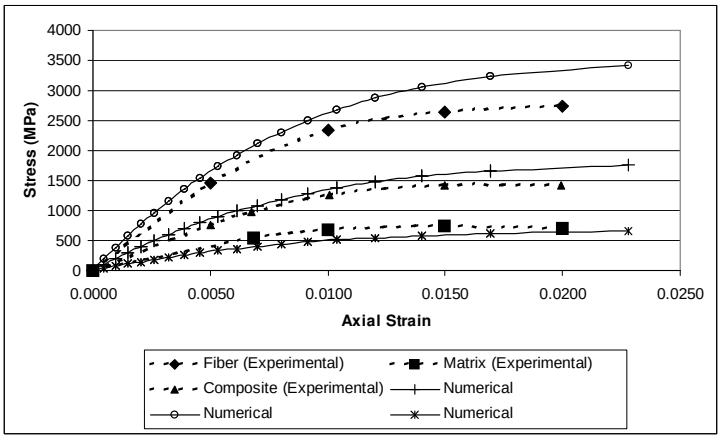

Figure 9: Comparison of numerical and experimental results for composite and components.

Example 5. Plate under pure shear. We consider the plate in figure 10. The plate is made with laminated material LTM45EL-SM [3], whose properties are given in Table 2. As the stress state is pure shear, only one of the parameters K_{ij} need to be determined ($K_{12} = 90$).

Experimental and numerical results may be seen in figure 11.

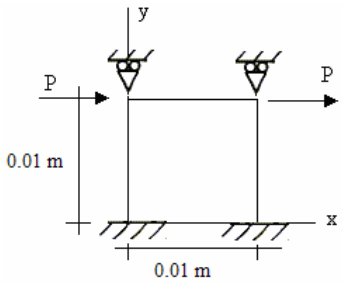

Figure 10: Geometry and loading

Table 2: Material properties for LTM45EL-SM

Properties	Fiber	Matrix	Laminate
Módulus E (GPa)	235.0	2.9	-
Poisson	0.2	0.38	0.3
G_{12}	96.311	0.760	4.0

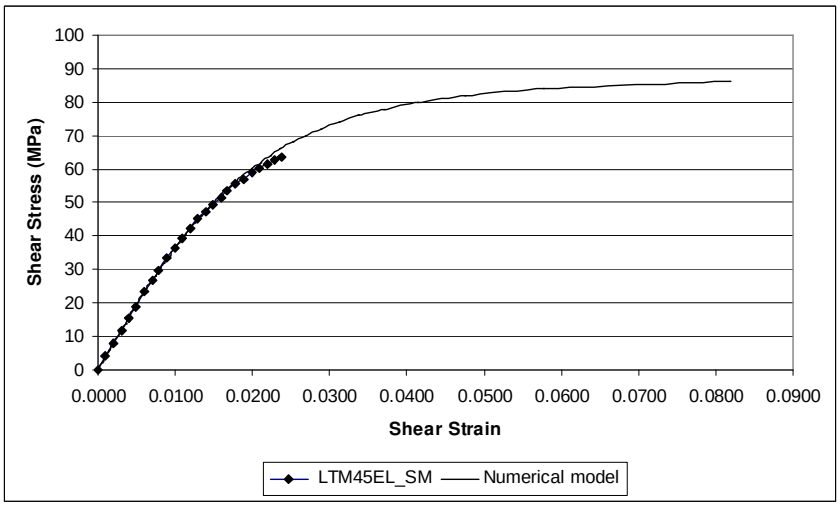

Figure 11: Comparison of model prediction and experimental data for shear of LTM45EL-SM unidirectional lamina

6 Conclusion and final remarks

Beginning with the fundamental hypotheses of Murakami [18, 19] and the damage matrix proposed by Voyiadjis & Kattan [23] the following results were obtained:

1. An incremental constitutive relation was determined and verified comparing numerical and analytical results.

2. This incremental relation was implemented into a Finite Element code for anisotropic shells.

3. The formulation and the code were validated for some simple states of stress comparing numerical and experimental results.

Moreover, the particular behavior of materials in the damaged state that leads to unloading and localization phenomena was described. This analysis shows the need of determining loading-unloading criteria and to face mesh-dependence effects. These important subjects will be addressed in a forthcoming paper.

Acknowledgements. The financial support of CAPES, PROPESQ, CNPq and UNOCHAPECÓ is gratefully acknowledged.

References

[1] E.J. Barbero. *Introduction to Composite Materials Design*. Taylor and Francis, Philadelphia, 1998.

[2] E.J. Barbero. Development and evaluation of glass fiber reinforced composites/wood railroad crossties phase ii task 5 continuous damage mechanics. Technical report, FRA, 1999.

[3] E.J. Barbero, G.F. Abdelal, and A. Caceres. A micromechanics approach for damage modeling of polymer matrix composites. *Composite Structures*, 67(427-436), 2005.

[4] K.J. Bathe. *Finite Element Procedures*. Prentice-Hall, 1996. Englewood Cliffs N.J.

[5] M. Brünig. An anisotropic continuum damage model: Theory and numerical analyses. *Latin American Journal of Solids and Structures*, 1:185–218, 2004.

[6] J.D. Eshelby, editor. *The Determination of the Elastic Field of an Ellipsoidal Inclusion and Related Problems*, volume A241. Royal Society, 1957. pp. 376-396.

[7] F.Desrumaux, F. Meraghni, and M.L. Benzeggagh. Generalised mori-tanaka scheme to model anisotropic damage using numerical eshelby tensor. Technical report, Université de Technologie de Compiègne; LG2mS—"Polymères & Composites, France, 2000.

[8] A.C. Gavazzi and D.C. Lagoudas. On the numerical evaluation of eshelby's tensor and its applications to elastoplastic fibrous composites. *Computational Mechanics*, 7:13–19, 1990.

[9] L.M. Kachanov. On the creep fracture time. Technical Report 8, Izv Akad. Nauk USSR Otd tekh, Dordrecht, 1958. pp. 26-31.

[10] L.M. Kachanov. *Introduction to Continuum Damage Mechanics*. Martinus Nijhoff Publishers, Dordrecht, 1986.

[11] D.C. Lagoudas, A.C. Gavazzi, and H. Nigam. Elastoplastic behavior of metal matrix composites based on incremental plasticity and the mori-tanaka averaging scheme. *Computational Mechanics*, 8:193–203, 1991.

[12] J. Lemaitre. How to use damage mechanics. *Nuclear Engineering and Design*, 80:233–245, 1984.

[13] J. Lemaitre. *A course on Damage Mechanics*. Springer-Verlag, Berlin, 1992.

[14] J. Lemaitre and J.L. Chaboche. *Mechanics of Solid Materials*. Cambridge University Press, London, 1990.

[15] Y. Liu, S. Murakami, and Y. Kanagawa. Mesh-dependence and stress singularity in finite element analysis of creep crack growth by continuum damage mechanics approach. *Eur. J. Mech.*, 13:395–417, 1994. A/Solids.

[16] S.P.C. Marques and G. J. Creus. Geometrically nonlinear finite elements analysis of viscoelastic composite materials under mechanical and higrothermal loads. *Computers and Structures*, 53:449–456, 1994.

[17] T. Mura. *Micromechanics of Defects in Solids*. Martinus Nijhoff Publishers, 1982.

[18] S. Murakami. Notion of continuum damage mechanics and its application to anisotropic creep damage theory. *Journal of Engineering Mechanics and Technology*, 105:99–105, 1983.

[19] S. Murakami. Mechanical modeling of material damage. *J. Appl. Mec.*, 55:280–286, 1988.

[20] B.F. Oliveira. Programa computacional para modelagem de cascas de materiais compostos com análise acoplada de viscoelasticidade e falhas progressivas. Master's thesis, PPGEC/UFRGS, 1999.

[21] F. Sidoroff. *Description of Anisotropic Damage Application to Elasticity; In IUTAM Colloquium on Physical Nonlinearities in Structural Analysis*. Springer-Verlag, Berlin, 1981. pp. 237-244.

[22] P.D. Soden, M. J. Hinto, and A.S. Kaddour. Lamina properties: lay-up configurations and loading conditions for a range of fibre-reinforced composite laminates. *Composites Science and Technology*, 58:1011–1022, 1998.

[23] G.Z. Voyiadjis and P.I. Kattan. *Advances in Damage Mechanics: Metals and Metal Matrix Composites*. Elsevier, Elsevier, 1999.

[24] G.J. Weng. Some elastic properties of reinforced solids with special reference to isotropic ones containing spherical inclusions. *International Journal of Engineering Science*, 22(845-856), 1984.

[25] Y. B. Yang and M. S. Shieh. Solution method for nonlinear problems with multiple critical points. *AIAA Journal*, 28:2110–2116, 1990.